PROCEEDINGS OF SCIENCE

Eigenvalue Distributions of the Dirac Operator at Finite Isospin Chemical Potential

Gernot Akemann
Department of Mathematical Sciences & BURSt Research Centre
Brunel University West London
Uxbridge UB8 3PH, United Kingdom
E-mail: gernot.akemann@brunel.ac.uk

Atsushi Nakamura
Hiroshima University
Hiroshima 739-8521, Japan
E-mail: nakamura@riise.hiroshima-u.ac.jp

Yuji Sasai*
Tsuyama National College of Technology
Okayama 708-8509, Japan
E-mail: sasai@tsuyama-ct.ac.jp

Tetsuya Takaishi
Hiroshima University of Economics
Hiroshima 731-0192, Japan
E-mail: takaishi@hiroshima-u.ac.jp

The comparison between unquenched SU(3) lattice QCD with chemical potential and random matrix theory can provide information on the pion decay constant F_π. We calculated eigenvalue distributions of the Dirac operator on a $8^3\times4$ lattice using $N_f = 2$ Kogut-Susskind fermions. We performed fits between the spectral density computed from random matrix theory and lattice data at coupling $\beta = 5.30$ for fixed quark mass $ma = 0.05$ and iso-vector chemical potential $\mu a = 0.0$, 0.004773, 0.1 and 0.2, finding good agreement. In particular our data indicate that F_π decreases as the iso-vector chemical potential increases. For a more precise fit of the rescaled parameter $\mu^2 F_\pi^2 V$ we also compare to the first eigenvalue distribution from random matrix theory.

The XXVI International Symposium on Lattice Field Theory
July 14 - 19, 2008
Williamsburg, Virginia, USA

*Speaker.

PoS(LATTICE 2008)181

1. Introduction

Lattice QCD with finite lattice spacing a in a 4-dimensional volume V is a powerful regularization method to obtain information about the non-perturbative regime. Baryon chemical potential μ_B inducing a finite quark density is relevant in the early universe, inside neutron stars or in heavy ion collisions. However, in SU(3) lattice QCD, the quark matrix becomes complex for $\mu_B \neq 0$ and this causes the famous sign problem. Thus ordinary Monte Carlo methods which generate gauge configurations with a Boltzmann weight, can not be used without modifications. Apart from the quenched approximation which disregards the Dirac determinant, there is the phase quenched method keeping the absolute value of the Dirac determinant in the measure[1], but disregarding its phase. In this case, an iso-spin chemical potential μ is being introduced. Within standard lattice QCD, we can still analyse the spectrum of such a theory for an even number of flavours N_f.

QCD in the ϵ-regime can be described using chiral Random Matrix Theory (RMT)[2]. RMT has produced many accurate analytical results. The most important observable is the spectral density of the Dirac operator. By comparing the spectral density to lattice data, one can determine low energy constants in the chiral Lagrangian: Σ, the chiral condensate, and F_π, the Pion decay constant. At $\mu = 0$, the Dirac operator is anti-Hermitian and its eigenvalues are distributed along the imaginary axis. But when $\mu \neq 0$, the spectrum extends into the complex plane. At this point the Dirac operator becomes non-Hermitian.

The spectral density correlation functions of quenched and unquenched Dirac operators at $\mu \neq 0$ were calculated using RMT by Splittorff and Verbaarschot[3], and by Osborn and coworkers [4, 5], respectively. Also the comparison between quenched QCD lattice data and the spectral density from RMT were done using Kogut-Susskind (KS) fermions[6] or overlap fermions[7]. The latter satisfy the Ginsparg-Wilson relation, maintaining an exact lattice chiral symmetry and exact zero-modes. They also satisfy an index theorem. However, overlap fermions require huge computational resources and it is difficult to accumulate enough unquenched gauge field configurations. For that reason we use unimproved KS fermions, which restricts us to the sector of trivial gauge topology.

At $\mu a \approx 0$, the spectrum close to the origin is oscillating along the imaginary axis, indicating the locations of individual eigenvalues. Consequently a fit between lattice QCD and chiral RMT can be done very accurately. However, these oscillation disappear rapidly as μa increases. Although a fit to the resulting plateau can be done, it becomes more convenient to compare to individual eigenvalue distributions. At $\mu = 0$, all individual eigenvalue distribution functions are known analytically[8]. When $\mu \neq 0$ individual eigenvalue distributions of the quenched and unquenched QCD Dirac operator can be calculated in an expansion[9].

In this article, we compare unquenched SU(3) lattice QCD data with iso-spin chemical potential to the spectral density and smallest eigenvalues of chiral RMT, and we also investigate the relationship between μa and F_π. In this comparison, it is important to define the mean level spacing d of the Dirac operator eigenvalues, in order to determine the rescaled quantities on the lattice. While at $\mu = 0$ this is obvious, at $\mu \neq 0$ the eigenvalue are distributed in two dimensions, and we evaluated d by projecting the complex eigenvalues onto the imaginary axis, using the Banks-Casher relation. Unfortunately it turns out that our rescaled quark mass is quite big, practically quenching the small eigenvalues. Our data are not yet fine enough to resolve the corresponding small difference between quenched and phase quenched RMT predictions.

2. Lattice Gauge Theory (LGT) and Random Matrix Theory (RMT)

At finite temperature our theory can be defined with the following partition function,

$$Z = \int DU\, D\bar{\psi}\, D\psi\, \exp[-\int_0^{1/k_BT} d\tau \int d^3x (L+\mu\bar{\psi}\gamma_4\psi)] = \int DU\, (\det\Delta(\mu))^{N_f/4}\, e^{-\beta S_g}\,. \tag{2.1}$$

Here, k_B stands for the Boltzmann constant, T for the temperature, N_f for the number of flavours, μ for the chemical potential, $\beta = 6/g^2$ for the coupling, S_g for the gauge action, and $\Delta(\mu)$ for the Dirac operator. We assign periodic (non-periodic) boundary conditions to the link (site) variables U (ψ) on the lattice, corresponding to the gauge (quark) fields.

In order to increase our statistics on the lattice, we use unimproved KS fermions, limiting us to gauge field topology $\nu = 0$. At $\mu = 0$, the fermion determinant $\det\Delta(\mu)$ is real and can be calculated. When $\mu \neq 0$, $\det\Delta(\mu)$ becomes complex, $|\det\Delta(\mu)|\, e^{i\theta}$ and the phase $e^{i\theta}$ invalidates the standard Monte Carlo formalism when updating gauge configurations. As a way out we consider the following phase quenched average $\langle O\rangle$, which is equivalent to introducing an iso-spin chemical potential for $N_f = 2$:

$$\langle O\rangle = \frac{1}{Z}\int DU\, |\det\Delta|^{1/2}\, O\, e^{-\beta S_g}\,. \tag{2.2}$$

In chiral RMT one writes the eigenfunctions of the Dirac equation in a chiral basis. The partition function of RMT at $\mu \neq 0$ defined as[4]

$$Z = \int dA\, dB\, \exp\{-N\,\mathrm{Tr}\,(AA^\dagger + BB^\dagger)\} \prod_{f=1}^{N_f} \det\begin{pmatrix} m_f & iA+\hat{\mu}B \\ iA^\dagger+\hat{\mu}B^\dagger & m_f \end{pmatrix}, \tag{2.3}$$

where A and B are $N\times N$ complex matrices for fixed topological charge $\nu = 0$, and $\hat{\mu}$ is the chemical potential in RMT. Because of chiral symmetry the $2N$ ($\sim$ Volume V) complex eigenvalues z_j come in $\pm$ pairs, we restrict the integration domain to the upper half-plane $\mathbb{C}_+$. Using a Schur decomposition of the RMT Dirac operator, we can define an eigenvalue basis where details are given in[4, 5]

$$Z = \prod_{j=1}^{N}\int_{\mathbb{C}_+} d^2z_j\, \mathcal{P}(\{z\})\,, \qquad \mathcal{P}(\{z\}) = \prod_{j=1}^{N} w^{(N_f)}(z_j) \prod_{i>j=1}^{N} \left|z_i^2 - z_j^2\right|^2\,. \tag{2.4}$$

Here $\mathcal{P}(\{z\})$ is the joint probability distribution function. The weight w depends on the N_f flavours and the quarks masses m_f ($f = 1,\ldots,N_f$),

$$w^{(N_f)}(z_j) = \prod_{f=1}^{N_f} (m_f^2 - z_j^2)\, |z_j|^2 K_0\left(\frac{N(1+\hat{\mu}^2)}{2\hat{\mu}^2}\,|z_j|^2\right) e^{\frac{N(\hat{\mu}^2-1)}{4\hat{\mu}^2}(z_j^2+z_j^{*2})}\,, \tag{2.5}$$

where K_0 is a modified Bessel function of the second kind.

The complex eigenvalue k-point distribution functions are defined as follows in RMT

$$R_k(z_1,\ldots,z_k) \equiv \frac{1}{Z}\frac{N!}{(N-k)!}\prod_{j=k+1}^{N}\int_{\mathbb{C}_+} d^2z_j\, \mathcal{P}(\{z\})\,, \tag{2.6}$$

e.g. $R_1(z)$ is the spectral density. All complex eigenvalue density functions can be computed as follows within the orthogonal polynomial method[4, 5],

$$R_k(z_1,\ldots,z_k) = \det_{1\le i,j\le k} \mathscr{K}_N(z_i,z_j^*). \tag{2.7}$$

Here $\mathscr{K}_N(z_i,z_j^*)$ is the kernel of bi-orthogonal polynomials expressed in terms of Laguerre polynomials in the complex plane.

In the microscopic large-N (volume) limit RMT becomes equivalent to QCD in the ϵ-regime[10]. In this limit we use the following RMT (Lattice) rescaling also called weak non-Hermiticity

$$\xi_i \equiv Nz_i (= V\Sigma z_i = z_i\pi/d)\,,\ \ \eta_f \equiv Nm_f (= V\Sigma m_f = m_f\pi/d)\,,\ \ \alpha^2 \equiv 2N\hat{\mu}^2 (= VF_\pi^2\mu^2)\,. \tag{2.8}$$

Here d is the mean level spacing based on Banks-Casher relation, as explained in the introduction. In the quenched case, the microscopic spectral kernel reads[3],

$$\mathscr{K}_s(\xi_1,\xi_2^*) = \frac{1}{2\pi\alpha^2}\,|\xi_1\xi_2|\,K_0(\frac{|\xi_1|^2}{4\alpha^2})^{\frac{1}{2}}\,K_0(\frac{|\xi_2|^2}{4\alpha^2})^{\frac{1}{2}}\exp[-\frac{\mathrm{Re}(\xi_1^2+\xi_2^2)}{8\alpha^2}]\int_0^1 dt\,e^{-2\alpha^2}I_0(\xi_1 t)\,I_0(\xi_2^* t), \tag{2.9}$$

where I_0 is a modified Bessel function of the first kind and the microscopic spectral density is $\hat{\rho}^{(N_f=0)}(\xi) = \mathscr{K}_s(\xi,\xi^*)$. For our phase quenched lattice data with $N_f = 2$ flavors of equal mass $\eta \equiv \eta_1 = \eta_2$, we also need the corresponding phase quenched result from RMT[4, 5]:

$$\hat{\rho}^{(N_f=2)}(\xi) = \hat{\rho}^{(N_f=0)}(\xi)\Big(1 - \frac{|\mathscr{K}_s(\xi,\eta^*)|^2}{\mathscr{K}_s(\eta,\eta^*)\,\mathscr{K}_s(\xi,\xi^*)}\Big). \tag{2.10}$$

3. Comparison of lattice data and RMT

In this section we compare the eigenvalue density function $\rho(\xi)$ of LGT and the microscopic spectral densities $\hat{\rho}^{(N_f=0,2)}(\xi)$ of RMT. In LGT, we generated the gauge configurations by using the R-algorithm with $N_f = 2$ fermions of mass $ma = 0.05$, on an $8^3\times 4$ lattice at $\beta = 5.30$. The next step is to calculate the eigenvalues for these gauge configurations. It is rather time consuming to calculate all eigenvalues using LAPACK. Since we only need the eigenvalues near the origin in the microscopic limit we only compute the first 100 eigenvalues ordered according to their absolute value. For this purpose, we use the LU decomposition and ARPACK. In this case, we calculated the eigenvalues for 5,000∼15,000 configurations since the calculation for each configuration can be done more quickly. Next, by taking the statistical average of these eigenvalue data, we obtained the eigenvalue density. In order to compare to RMT notation, the eigenvalue density function was normalised as $\int d\xi\hat{\rho}(\xi) = N = N_c\times 8^3\times 4$.

Table 1: Summary of simulation parameters (β=5.30, V=8^3×4)

μa	level spacing d	no. of config.
0.0	$2.57(4)\times10^{-3}$	5,000
0.004773	$2.64(4)\times10^{-3}$	15,000
0.10	$2.73(4)\times10^{-3}$	15,000
0.20	$4.3(2)\times10^{-3}$	10,000

For the comparison of the lattice data and RMT, the mean level spacing d plays an important role. At $\mu a = 0$, the eigenvalues lie on the imaginary axis. In order to obtain the eigenvalue density near the origin in the Banks-Casher relation $\Sigma = \langle\bar{\psi}\psi\rangle = -\pi\rho(0)/V = -\pi/(Vd)$, we need the spacing d

of the eigenvalues along the imaginary axis. At $\mu a \neq 0$, the problem of defining an order occurs because the complex eigenvalues spread into two dimensions. Because we consider weak non-Hermiticity, we project the complex eigenvalues on the imaginary axis and measure d of several eigenvalues near the origin. At $\mu a = 0.0,\ 0.004776$ and 0.1 the variation of d due to the number of minimum eigenvalues is small, but for larger μa, the variation of d increases.

In the case of the chemical potential $\mu a = 0.1$, we investigate the relationship between LGT and RMT as follows.

1. Calculation of the mean level spacing d and rescaling of the lattice data: We have 15,000 configurations and we calculate the average mean level spacings of the smallest 7 eigenvalues in each configuration. This results to a value $d = 2.73(4)\times10^{-3}$ then being used in rescaling the eigenvalue za with $\pi/d = 1.15(2)\times10^{3}$, leading to rescaled eigenvalues ξ (see eq. (2.8)).

2. The rescaled mass obtained from ma in the same way reads $\eta = 57.6$. Up to this point we have no free parameter.

3. Using this value for η we choose α to fit best eq. (2.10) from RMT. In order to do a one-dimensional fit we choose a cut of the density along the real axis, leading to $\alpha = 1.68$. The same values of α is then used for the quenched and phase quenched curve in Fig. 2.

As shown in Fig. 2, the phase quenched LGT result and RMT results coincide with tuning only one free parameter α. Because the effect of unquenching is very small due to $\eta \gg 1$, our data cannot distinguish between quenched and phase quenched RMT predictions, being consistent with both curves. For comparison we also show the histogram of first, second, and third eigenvalue of the lattice data.

In the case of $\mu a = 0.2$, Fig. 3 shows the comparison between the lattice QCD data and RMT. Based on the RMT curves it is obvious that the quark mass pushes the density in along the real axis. Although the difference between quenched and phase quenched is most pronounced for this value of μa, it is still not conclusive for our data. Moreover, for this μa we have β=5.30 $\approx \beta_c$=5.29(9) from the simulation of Kogut and Sinclair [11], so we are on the chiral phase transition to the deconfined

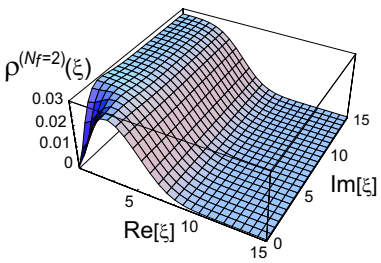

Figure 1: RMT density eq. (2.10) at $\alpha = 1.68$ and $\eta = 57.6$.

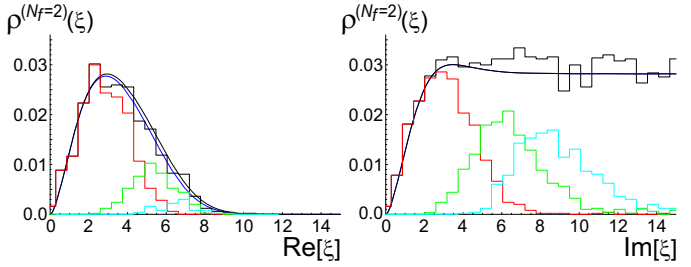

Figure 2: The eigenvalue density at $\mu a = 0.10$ cut along the real axis (left) and the imaginary axis (right). The histograms in black are unquenched lattice data. Red, green and light-blue histograms stand for the first, the second and the third lattice eigenvalue distributions. The blue (black) curve corresponds to the unquenched (quenched) RMT result for $\alpha = 1.68$ and $\eta = 57.6(\infty)$.

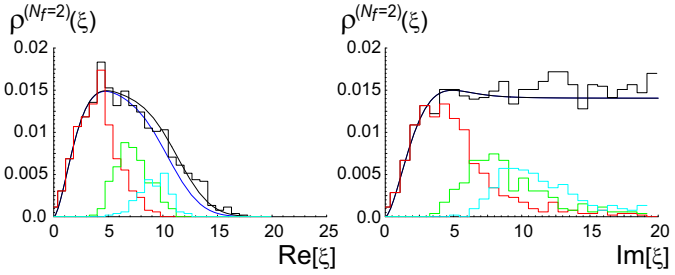

Figure 3: Same as Fig.2, but for $\mu a = 0.20$, $\alpha = 2.38$ and $\eta = 36.2$.

Table 2: Estimation of F_π as μa increases.

μa	α_{fit}	$\alpha_{fit}/\mu a$
0.0	none	none
0.004773	0.08	16.8
0.10	1.68	16.8
0.20	2.38	11.9

phase, where the RMT used no longer applies. The agreement with the data still looks remarkably good. Following [11] we keep our $\mu a < m_\pi a/2 \approx 0.29$ away from the pion condensation transition.

Let us now comment on F_π as a function of μ. By calculating $\alpha/\mu a = F_\pi/\sqrt{V}$, it is possible to estimate the variation of Pion decay constant F_π with μ. The result is shown in Table2. At $\mu a = 0.0, 0.004773$ and 0.10, the coupling constant $\beta = 5.30$ is smaller than β_c and these density regions are in the confined phase. Also, the chiral condensate $\langle\bar{\psi}\psi\rangle$ and $\alpha_{fit}/\mu a$ do not change so much. But at $\mu a = 0.20$ (on or above the transition), $\langle\bar{\psi}\psi\rangle$ and $\alpha_{fit}/\mu a$ decrease. This points out that F_π decreases as μ reaches close to μ_c.

4. First eigenvalue distribution for complex eigenvalues from RMT

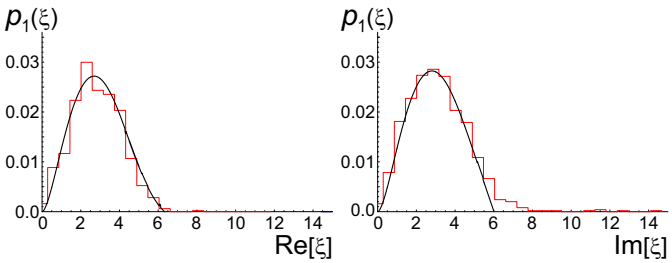

Figure 4: First eigenvalue distribution at $\mu a = 0.10$. The red histogram stands for the first eigenvalue density distribution from phase quenched LGT, the black curve is the corresponding distribution $p_1(\xi)$ from quenched RMT.

In the small-μa region, the oscillations present in the eigenvalue density $\rho(\xi)$ of LGT and $\hat{\rho}(\xi)$ of RMT facilitate an accurate fit. As μa increases, the oscillations disappear and a simple plateau appears. Thus it becomes important to compare to individual eigenvalue distributions. From the relation between the gap probability and 1st eigenvalue $p_1(\xi)$, we can express the latter in a expansion of density distributions[9],

$$p_1(\xi) = R_1(\xi) - \int_J d\xi' R_2(\xi,\xi') + \frac{1}{2}\int_J d\xi' d\xi'' R_3(\xi,\xi',\xi'') + \cdots . \tag{4.1}$$

Here 1 eigenvalue is inside the set J, and $N-1$ eigenvalues are in its complement $\bar{J} \equiv \mathbb{C}_+/J$. Eq.(2.9) gives the quenched microscopic one- and two-point functions as follows,

$$\hat{\rho}^{(N_f=0)}(\xi) = \mathscr{K}_s(\xi,\xi^*), \qquad \hat{\rho}^{(N_f=0)}(\xi,\xi') = \mathscr{K}_s(\xi,\xi^*)\mathscr{K}_s(\xi',\xi'^*) - \mathscr{K}_s(\xi,\xi'^*)\mathscr{K}_s(\xi',\xi^*). \tag{4.2}$$

In the case of $\mu a = 0.10$ a preliminary comparison is made between the first eigenvalue density $p_1(\xi)$ of LGT and quenched RMT, as shown in Figure 4. Only the first two terms were used in the expansion Eq. (4.1) due to the convergence time of the calculation. The agreement between lattice data and RMT analytical curve is good up to almost $\mathrm{Im}(\xi) \approx 6.0$ where our approximation breaks down and we have cut the curve becoming negative.

5. Summary

We have performed unquenched simulations on a $8^3 \times 4$ lattice using $N_f = 2$ flavours of Kogut-Susskind fermions at mass $ma = 0.05$, for several values of an iso-spin chemical potential μa. To analyze distributions of the Dirac eigenvalues we compared to prediction from RMT for the density and individual eigenvalues, being valid in the ϵ-regime of QCD. In the case of $\mu a = 0.0$ there is no free parameter and we found excellent agreement up to including the first three eigenvalues. For values $\mu a = 0.004773, 0.10$ and 0.20, it was possible to fit to the RMT curves by tuning one parameter $\alpha^2 = \mu^2 F_\pi^2 V$, thus determining the pion decay constant. We estimated the variation of F_π with μa, finding a decrease from the confined phase compared to $\mu a = 0.20 \approx \mu_c a$ approximately on the chiral phase transition. Unfortunately our quark masses were too large to find a sizable difference between quenched and phase quenched predictions of RMT. Our data were in good agreement though and consistent with both curves for all values of chemical potential, including up to $\mu_c a$.

Acknowledgments

The simulations were performed on SX-8 (NEC) at RCNP of Osaka University and on SR-11000 (Hitachi) of Hiroshima University. This work was supported by the JSPS Grant-in-Aid for Scientific Research No.20500769, No.17340080, No.20340055, EPSRC grant EP/D031613/1, and European Network ENRAGE MRTN-CT-2004-005616.

References

[1] S. Muroya, A. Nakamura, C. Nonaka and T. Takaishi, Prog. Theor. Phys.**110** (2003) 615 [hep-lat/030631] ; A. Nakamura, Y. Sasai and T. Takaishi, Nucl. Phys. (Proc. Suppl.) **129-130C** (2004) 539 [hep-lat/0310046] ; A. Nakamura, Y. Sasai and T. Takaishi, AIP Conf. Proc. **756** (2005) 416.

[2] E. V. Shuryak and J. J. M. Verbaarschot, Nucl. Phys. **A560** (1993) 306 [hep-th/9212088]; J.J.M. Verbaarschot, Phys. Rev. Lett. **72** (1994) 2531 [hep-th/9401059].

[3] K. Splittorff and J.J.M. Verbaarschot, Nucl. Phys. **B683** (2004) 467 hep-th/0310271].

[4] J. C. Osborn, Phys. Rev. Lett. **93** (2004) 222001 [hep-th/0403131].

[5] G. Akemann, J.C. Osborn, K. Splittorff and J.J.M. Verbaarschot, Nucl. Phys. **B712** (2005) 287 [hep-th/0411030].

[6] G. Akemann and T. Wettig, Phys. Rev. Lett. **92** (2004) 102002 [Erratum-ibid. **96** (2006) 029902] [hep-lat/0308003]; J.C. Osborn and T. Wettig, PoS **LAT2005** (2006) 200 [hep-lat/0510115].

[7] J. Bloch and T. Wettig, Phys. Rev. Lett. **97** (2006) 012003 [hep-lat/0604020].

[8] S.M. Nishigaki, P.H. Damgaard and T. Wettig, Phys. Rev. **D58** (1998) 087704 [hep-th/9803007]; P.H. Damgaard and S.M. Nishigaki, Phys.Rev. **D63** (2001) 045012 [arXiv:hep-th/0006111v2].

[9] G. Akemann, J. Bloch, L. Shifrin and T. Wettig, Phys. Rev. Lett. **100** (2008) 032002 [arXiv:0710.2865v2 [hep-lat]]; PoS **LAT2007** (2007) 224 [arXiv:0711.0629 [hep-lat]].

[10] P.H. Damgaard, J.C. Osborn, D. Toublan, and J.J.M. Verbaarschot, Nucl. Phys. **B547** (1999) 305 [hep-th/9811212]; F. Basile and G. Akemann, JHEP **12** (2007) 043 [arXiv:0710.0376 [hep-th]].

[11] J.B. Kogut and D.K. Sinclair, Phys. Rev. **D70** (2004) 094501; [hep-lat/0407027].